ACS OMEGA

http://pubs.acs.org/journal/acsodf

Article

Versatile and Sustainable Approach to Access Biologically Relevant Chromeno[2,3-*b*]pyridine and Benzylpyrazolyl Coumarin Derivatives Using Graphitic Carbon Nitride as a Reusable Heterogeneous Catalyst

Sushmita Gajurel,[†] Rajib Sarkar,[†] Fillip Kumar Sarkar, Lenida Kyndiah, and Amarta Kumar Pal*

Cite This: *ACS Omega* 2022, 7, 48087−48099

Read Online

ACCESS | Metrics & More | Article Recommendations | Supporting Information

ABSTRACT: Herein, the synthesis of graphitic carbon nitride (g-C_3N_4) via the simple heating of cheap and readily available urea as the starting material has been reported. The catalytic activity of the prepared g-C_3N_4 was investigated for the synthesis of chromeno[2,3-*b*]pyridine and benzylpyrazolyl coumarin derivatives in an ethanol medium. The reactions were performed under mild conditions to achieve widely functionalized target products in a one-pot operation. The as-synthesized g-C_3N_4, being a heterogeneous catalyst, demonstrates excellent recyclability up to the 5th consecutive run without a significant decrease in its catalytic activity and yield of the product. A gram-scale reaction was performed to demonstrate the industrial applications of the present protocol. The green chemistry metrics such as environmental factor (E-factor), atom economy (AE), carbon efficiency (CE), and reaction mass efficiency (RME) were calculated and found to be very close to the ideal values. Additionally, operation simplicity, wide substrate scope, easy reusability of the catalyst, and avoidance of metal contamination in the products drive the process toward green and sustainable development.

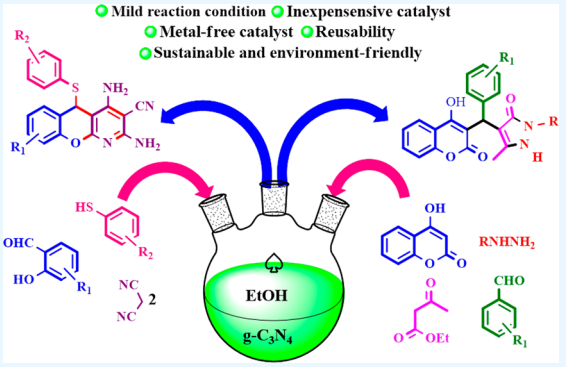

INTRODUCTION

The growing interest in graphitic carbon nitride (basically composed of carbon and nitrogen groups) in the arena of catalysis has contributed enormously to the research community in recent times.[1] This metal-free and polymeric natured g-C_3N_4 has emerged with an intense area of research, which embraces outstanding features owing to its high chemical and thermal stability, extreme hardness, base-functionalized surface, good photocatalytic character, and earth abundancy.[2−5] The tri-s-triazine unit as well as the high thermal and hydrothermal stability possessed by the structure of graphitic carbon nitride makes it insensitive to acidic and alkaline atmospheres as well.[5−8] Moreover, it possesses Lewis and Bronsted basic functionalities, π-bonds, and a functionalized N-rich group that render it a promising catalyst and catalyst support for many organic transformations. Besides its catalytic behavior, it has applications in solar cells, optical devices, biomedicines, etc.[9−11] Owing to its astounding properties, graphitic carbon nitride, through its exotic performances, has emerged to be a prominent catalyst in replacing innumerable mundane methods of organic synthesis. Moreover, it has been an attractive candidate to complement graphene in catalytic aspects.[4] Furthermore, some of the reported notable reactions catalyzed by g-C_3N_4 are oxygen reduction,[12] transesterifications,[13] photodegradation of dyes,[14] and hydrogen production.[8,15] However, the application of graphitic carbon nitride in multicomponent reactions is an emerging area yet to be explored vigorously whose benefits might lead to never-ending synthetic practice.

Chromeno[2,3-*b*]pyridine, a fused heterocyclic compound primarily consisting of chromene and a pyridine ring in a single molecule, has captivating features, motivating researchers to perform a considerable number of studies.[16] These heterocycles are endowed with significant biological properties such as antibacterial, antiproliferative, antirheumatic, antiarthritic, antiasthmatic, hypotensive, and chemotherapeutic properties.[17−22] Few among many of the reported biologically active chromeno[2,3-*b*]pyridine libraries have been illustrated in Figure 1. Several synthetic methodologies are emerging for the synthesis of chromeno[2,3-*b*]pyridines, but minimum synthetic reports are available utilizing salicylaldehydes, malononitrile, and thiophenols as precursors. Moreover, these reported synthetic procedures for chromeno[2,3-*b*]pyridines rely on a

Received: September 20, 2022
Accepted: November 30, 2022
Published: December 13, 2022

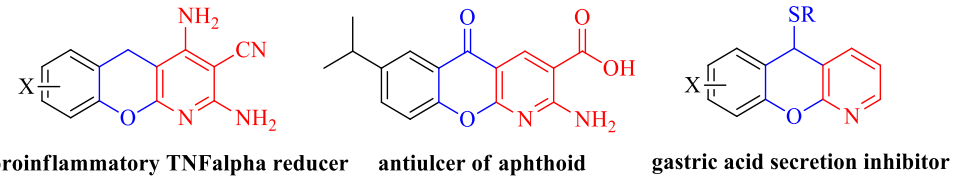

Figure 1. Biologically active chromeno[2,3-*b*]pyridines.

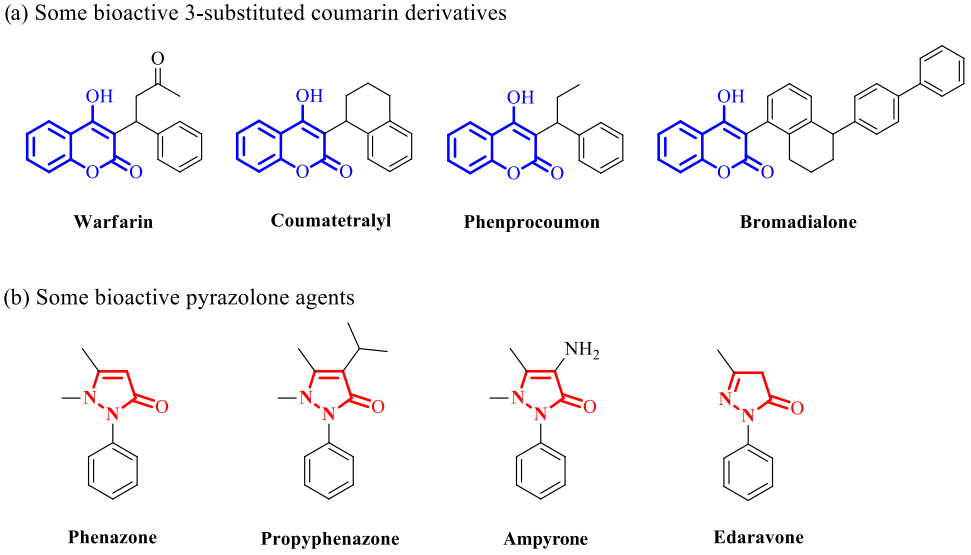

Figure 2. Structures of some selected biologically relevant (a) coumarin- and (b) pyrazolone-based compounds.

Scheme 1. Schematic Representation of the Synthesis of g-C_3N_4

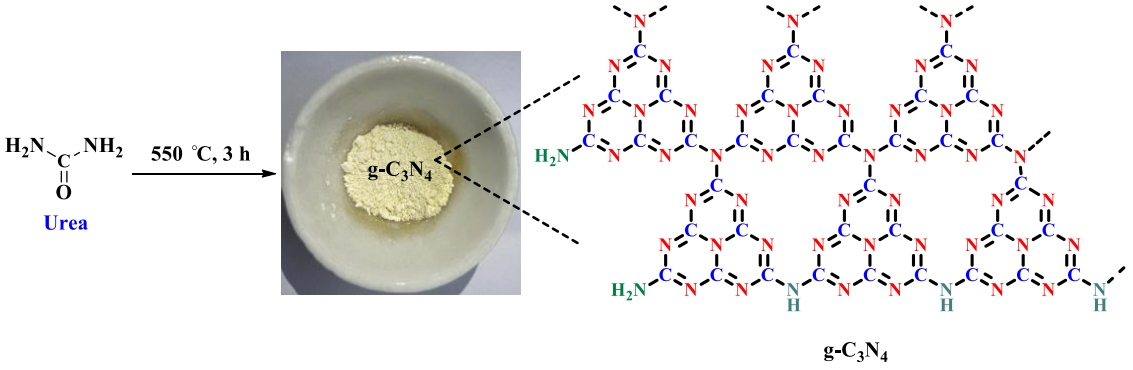

method based on harsh and uneconomical reaction conditions, such as usage of a metal catalyst such as ZrP_2O_7[23] or SnO,[24] employment of a base such as Et_3N[25] or K_2CO_3,[26] and usage of an acid like chitosan-functionalized citric acid[27] as a catalyst, resulting in prolonged reaction time and difficulty in catalyst separation and recyclability. These drawbacks in these methodologies necessitate a new, greener, and sustainable method to eliminate the traditional practice.

Likewise, pyrazolones and 3-substituted 4-hydroxycoumarin, particularly 3-benzyl substituted 4-hydroxycoumarin derivatives, assemble in the main core structure of various medically viable drug molecules present in various natural products.[28] Warfarin, coumatetralyl, carbochromen, phenprocoumon, and bromadialone (Figure 2a) are some of the important 3-substituted 4-hydroxycoumarin scaffolds that exist in many natural products and exhibit various biological activities such as anticoagulant,[29] anti-HIV,[30] antiviral,[31] antioxidant,[32] and anticancer activities.[33] Similarly, the pyrazolone nucleus is a prominent pharmacophore that manifests a broad spectrum of pharmacological properties such as antitumor, anti-inflammatory, antibacterial, gastric secretion stimulatory, analgesic, and antipyretic properties.[34−38] Edaravone (MCI-186) is a food and drug administration (FDA)-approved pyrazolone drug used for the treatment of ischemic stroke and amyotrophic lateral sclerosis (ALS) (Figure 2b). Additionally, they also act as a potent Chk1 kinase inhibitor.[39−41] Therefore, a single nucleus constituting both 3-benzyl substituted 4-hydroxycoumarin and pyrazolone moieties might lead to some integrated biological properties in synthetic medicinal chemistry. To date, only a few methodologies have been reported for the development of such benzylpyrazolyl coumarin derivatives. However, the major disadvantages of these protocols are the use of corrosive and unrecyclable homogeneous acid catalysts like glacial acetic acid,[42] 2-aminoethanesulfonic acid,[43] $Ca(OTf)_2$,[44] and $NbCl_5$[45] and the use of expensive heterogeneous catalysts like ZrO_2 nanoparticles[28] and Nb-Zr/KIT-6.[46]

https://doi.org/10.1021/acsomega.2c06070
ACS Omega 2022, 7, 48087−48099

Therefore, the synthesis of such aforementioned biologically relevant heterocyclic compounds by the combination of MCR and carbon-based metal-free catalysts would be highly desirable. In this article, we demonstrated the catalytic application of g-C_3N_4 as a metal-free heterogeneous catalyst for the synthesis of chromeno[2,3-*b*]pyridines and benzylpyrazolyl coumarin derivatives via a one-pot multicomponent reaction under sustainable conditions.

RESULTS AND DISCUSSION

Graphitic carbon nitride has been synthesized and characterized by various spectroscopic techniques such as Fourier transmission infrared spectroscopy (FT-IR), scanning electron microscopy (SEM), transmission electron microscopy (TEM), energy-dispersive X-ray spectroscopy (EDX), powdered X-ray diffraction (PXRD), and thermogravimetric analysis (TGA). The schematic representation of the preparation of graphitic carbon nitride is shown in Scheme 1.

FT-IR spectroscopy was carried out to analyze the functional groups of as-synthesized graphitic carbon nitride (Figure 3).

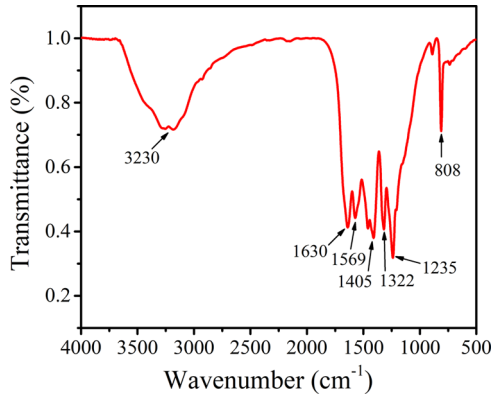

Figure 3. FT-IR spectrum of g-C_3N_4.

The FT-IR spectrum of g-C_3N_4 showed intense bands at 1630 and 1569 cm^{-1} corresponding to the stretching vibration of the C═N group. Other bands obtained at 1405, 1322, and 1235 cm^{-1} can be ascribed to the aromatic C−N stretching vibrations. A sharp band observed at 808 cm^{-1} corresponds to the repeating units of triazine moieties in graphitic carbon nitride. Furthermore, the broad bands obtained at 3285−3161 cm^{-1} can be assigned to the stretching of $-NH_2$ or ═NH groups in the graphitic carbon nitride.[47]

Furthermore, the morphology of the prepared graphitic carbon nitride was investigated by SEM and TEM analyses, and the obtained images are shown in Figure 4. The SEM image of g-C_3N_4 (Figure 4a) shows a collapsed and agglomerated sheet-like crumbled structure. The TEM images (Figure 4b,c) show a close-packed sheet-like morphology, and the obtained results are in good agreement with the reported ones.[48] The selected-area electron diffraction (SAED) pattern shown in Figure 4d shows the amorphous nature of the catalyst. Figure 4e shows the EDX spectrum of g-C_3N_4, which distinctly shows the presence of constituent elements such as carbon and nitrogen in the prepared g-C_3N_4 catalyst.

The PXRD pattern of g-C_3N_4 shows a strong peak at 13.1 and 27.4°, which agrees with the reported values corresponding to the (100) and (002) diffraction planes, as shown in Figure 5a.[49] The thermal stability of the prepared graphitic carbon nitride was also investigated by thermogravimetric analysis (TGA), and the obtained result is presented in Figure 5b. From Figure 5b, the first break in the curve at 150 °C is expected due to the intercalated water molecules present in the synthesized g-C_3N_4. The major break in the curve is noticed from 502 to 744 °C, which displays the decomposition of the graphitic carbon nitride framework, which is also in good agreement with the literature.[48,50] Therefore, in terms of thermal stability, graphitic carbon nitride is expected to be highly stable and can be used below 500 °C.

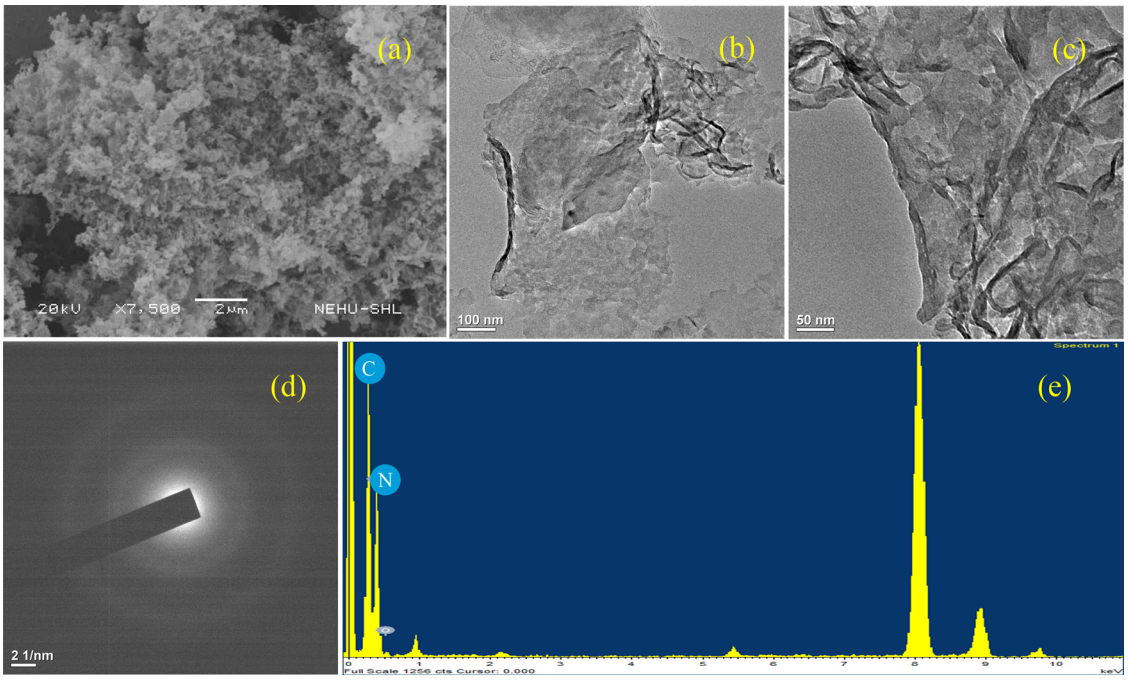

Figure 4. SEM image (a), TEM images (b, c), SAED pattern (d), and EDX image (e) of g-C_3N_4.

https://doi.org/10.1021/acsomega.2c06070
ACS Omega 2022, 7, 48087−48099

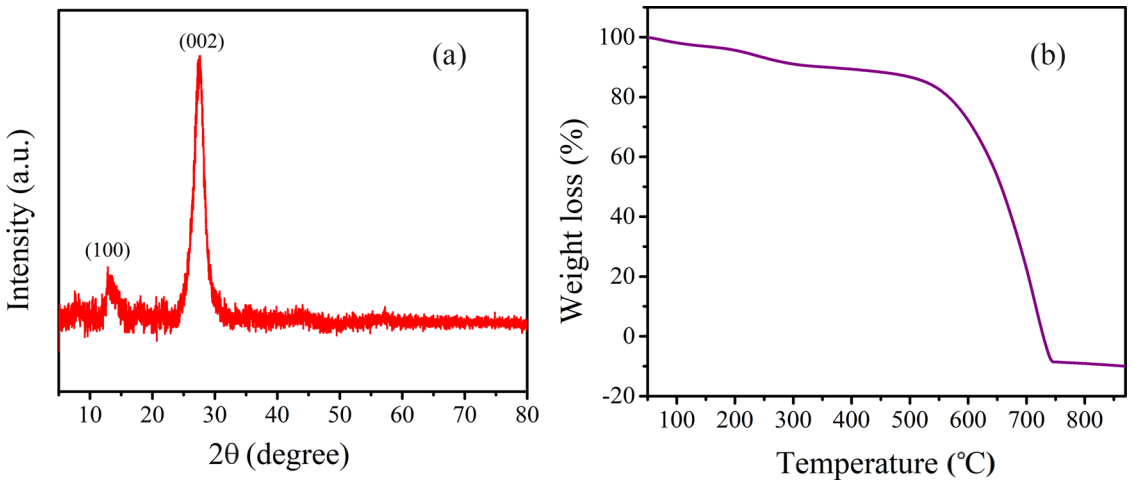

Figure 5. PXRD pattern (a) and TGA thermogram (b) of g-C_3N_4.

As the aim for the successful synthesis of the catalyst was accomplished by the above-supported characterization data, the catalytic property of g-C_3N_4 was scrutinized via a one-pot, multicomponent synthesis of chromeno[2,3-*b*]pyridine derivatives. In the initial study, the prospective of the catalyst was analyzed by executing salicylaldehyde (1 mmol), malononitrile (2 mmol), thiophenol (1 mmol), and g-C_3N_4 under different reaction conditions (Table 1). The detailed investigation for the optimization of the solvent, time, and temperature has been thoroughly illustrated in Table 1. A blank experiment was performed without the catalyst at room temperature (25 °C) applying EtOH as the solvent for 10 h, and no product formation was observed. Again, the same reaction was performed under the reflux condition, which rendered 17% yield of chromeno[2,3-*b*]pyridine in 3 h. Therefore, realizing the need of a catalyst, the model reaction was set with g-C_3N_4 in ethanol. It is of note that, on increasing the reaction temperature from 25 °C to reflux, the yield of the reaction enhanced proportionally. A maximum of 84% yield was noticed under the reflux condition for 3 h. The reaction time was also increased to 4 h, but no increment in the product yield was noticed and the yield was found to be 84%. Then, the effects of various solvents such as dimethylformamide (DMF), 1, 4-dioxane, H_2O, ethylene glycol, and poly(ethylene glycol) (PEG-400) on product yields were scrutinized under the heating condition (Table 1). H_2O, DMF, and 1,4-dioxane provided unsatisfactory yields (20, 19, and 22%) at 100 °C. Furthermore, green solvents such as EG and PEG-400 resulted in good yields of the products at 100 °C, i.e., 74 and 78%, respectively (Table 1). Under the solvent-free reaction condition (SFRC), only 30% yield of the desired product was obtained at 80 °C. Therefore, EtOH was chosen as the solvent of choice. Again, envisaging the catalyst concentration, it was found that 10 mg would be the established condition of the catalyst concentration (Table 1). Low catalyst loading (2−8 mg) produced less yields, but no improvement was noticed with a high catalyst loading (12 mg). Furthermore, several other catalysts such as L-proline, sodium acetate (NaOAc), Cs_2CO_3, and urea were examined for the model reaction, which produced the product in 46, 28, 48, and 32% yields, respectively (Table 2). Furthermore, the structure of compound **4a** was established by analyzing FT-IR, ^1H, and ^{13}C NMR spectroscopies.

With the optimized reaction conditions in hand, we then examined the scope and generality of the reaction to synthesize diversely functionalized chromeno[2,3-*b*]pyridine derivatives using various salicylaldehydes (both substituted and unsubstituted), thiophenols (substituted and unsubstituted), and benzyl thiol; the results are presented in Table 3. Salicylaldehyde with no substitution was found to undergo the reaction smoothly and afforded the corresponding products **4a** and **4b** in 84 and 87% yields, respectively (Table 3). Similarly, salicylaldehyde, bearing both electron-

Table 1. Optimization of Reaction Conditions for the Synthesis of Chromeno[2,3-*b*]pyridine Derivatives[a]

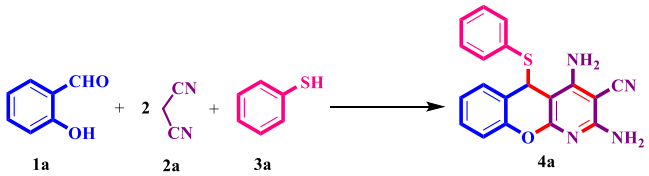

1a 2a 3a 4a

entry	catalyst (mg)	solvent	temperature (°C)	time (h)	yield (%)[b]
1	nil	EtOH	25	10	nil
2	nil	EtOH	reflux	3	17
3	10	SFRC	80	3	30
4	10	DMF	100	3	19
5	10	1,4-dioxane	100	3	22
6	10	H_2O	100	3	20
7	10	PEG-400	100	3	78
8	10	EG	100	3	74
9	10	EtOH	reflux	3	84
10	10	EtOH	25	24	32
11	10	EtOH	40	3	trace
12	10	EtOH	60	3	42
13	10	EtOH	reflux	2	58
14	10	EtOH	reflux	4	84
15	12	EtOH	reflux	3	84
16	8	EtOH	reflux	3	78
17	6	EtOH	reflux	3	74
18	4	EtOH	reflux	3	68
19	2	EtOH	reflux	3	51

[a]Reaction conditions: salicylaldehyde (**1a**, 1 mmol), malononitrile (**2a**, 2 mmol), thiophenol (**3a**, 1 mmol), g-C_3N_4, and solvent (5 mL). [b]Isolated yield.

https://doi.org/10.1021/acsomega.2c06070
ACS Omega 2022, 7, 48087−48099

Table 2. Comparison of Different Catalysts[a]

entry	catalyst (10 mg)	time (h)	yield (%)[b]
1	L-proline	3	46
2	NaOAc	3	28
3	Cs_2CO_3	3	48
4	urea	3	32
5	g-C_3N_4	3	84

[a]Reaction conditions: salicylaldehyde (**1a**, 1 mmol), malononitrile (**2a**, 2 mmol), thiophenol (**3a**, 1 mmol), catalyst (10 mg), and EtOH (5 mL). [b]Isolated yield.

donating and electron-withdrawing groups, was also found to react well and furnished the products in good yields (Table 3). However, disubstituted salicylaldehyde such as 3,5-dichlorosalicylaldehyde showed a slightly lower reactivity and gave the corresponding products (**4i** and **4j**) in 76 and 77% yields (Table 3). On the other hand, benzyl thiol reacted slowly and offered a slightly lower yield of the desired products (**4g**, **4h**, and **4m**, Table 3) compared to aromatic thiols bearing electron-donating groups or no substitution. The detailed characterization data of the compounds (**4a**–**n**) are presented in the Supporting Information.

To describe the sustainability and impact of the present protocol on the environment, some of the green chemistry

Table 3. Synthesized Chromeno[2,3-*b*]pyridine Derivatives[a,b]

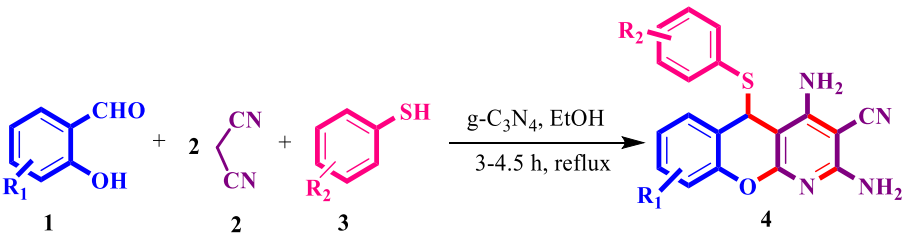

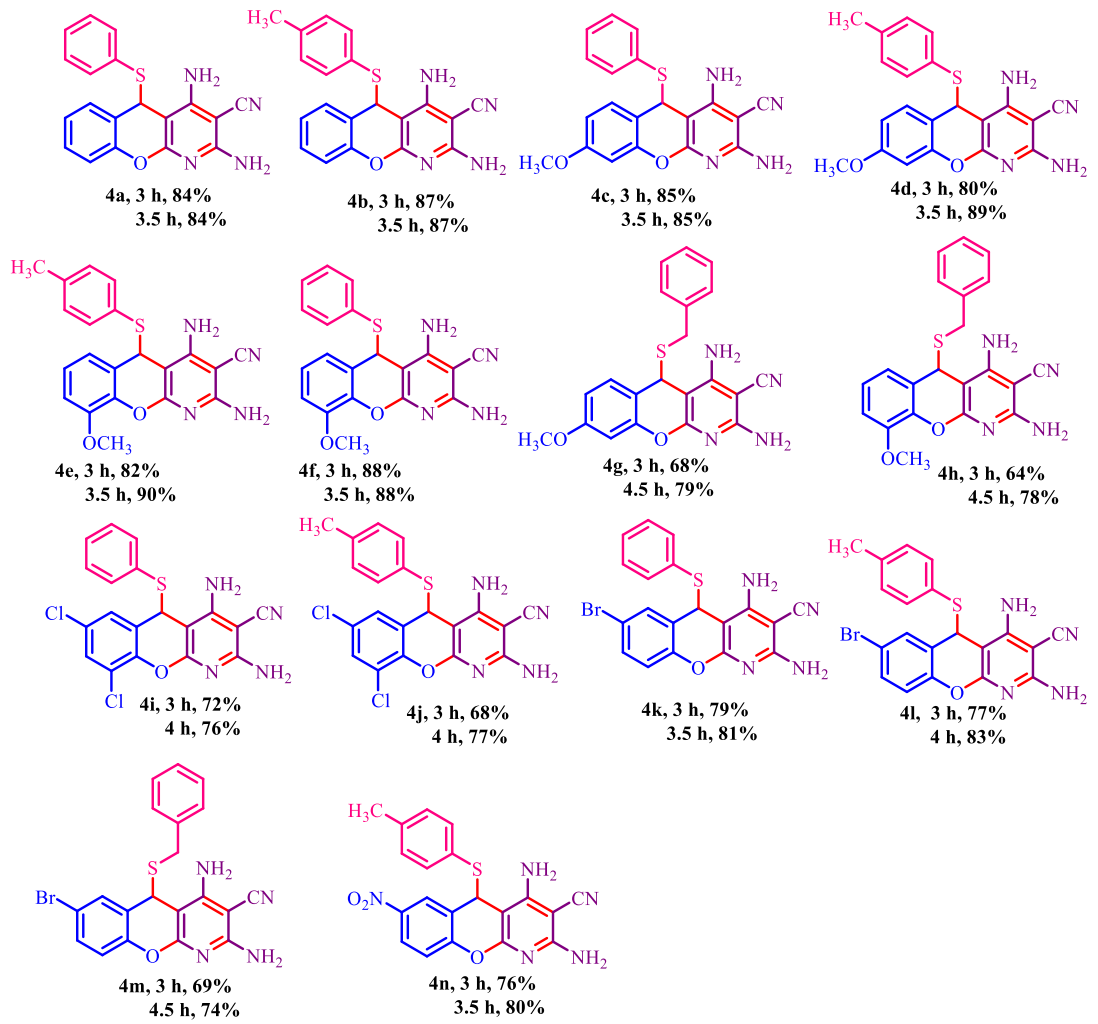

[a]Reaction conditions: salicylaldehyde (**1**, 1 mmol), malononitrile (**2**, 2 mmol), thiophenol (**3**, 1 mmol), g-C_3N_4 (10 mg), and EtOH (5 mL) were refluxed for 3–4.5 h under constant stirring. [b]Isolated yield.

https://doi.org/10.1021/acsomega.2c06070
ACS Omega 2022, 7, 48087−48099

metrics such as environmental factor (E-factor), atom economy (AE), carbon efficiency (CE), and reaction mass efficiency (RME) were analyzed for one of the synthesized compounds (**4a**) under the optimized reaction condition (Table 1), and it was found to possess close values with the ideal green chemistry metrics. The obtained results are presented in Table 4 (the detailed calculation is provided in the Supporting Information).

Table 4. Calculation of Green Chemistry Metrics

serial no.	green chemistry metrics	ideal value	product (**4a**)
1	E-factor	0	0.25
2	atom economy (AE)	100%	95%
3	carbon efficiency (CE)	100%	84%
4	reaction mass efficiency (RME)	100%	80%

Proposed Mechanism of the Reaction. A suitable mechanistic pathway has been proposed for graphitic carbon nitride catalyzed one-pot synthesis of chromeno[2,3-*b*]pyridine derivatives (Scheme 2). It was supposed that the primary amine groups of graphitic carbon nitride facilitated the reaction between salicylaldehyde (**1**) and malononitrile (**2**) through Knoevenagel condensation to form the intermediate (**I**), which undergoes intramolecular cyclization to furnish the iminochromene intermediate (**II**). On the other hand, g-C_3N_4 converts thiophenols or benzyl thiols to their corresponding thiophenoxide ions by abstraction of the −SH proton. This thiophenoxide anion then attacks iminochromene via the Michael fashion and generates the phenylsulfanyl chromene (**IV**) intermediate. Again, phenylsulfanyl chromene (**IV**) was reacted with another malononitrile molecule (**2**) to produce the intermediate (**V**). Aromatization of the piperidine ring of intermediate (**V**) afforded the desired chromeno[2,3-*b*]-pyridines (**4**).

Gram-Scale Synthesis of Chromeno[2,3-*b*]pyridine. To display the industrial application of the present protocol, gram-scale synthesis of chromeno[2,3-*b*]pyridine was explored (Scheme 3). A typical experiment was carried out by reacting salicylaldehyde (**1a**, 10 mmol), malononitrile (**2a**, 20 mmol), thiophenol (**3a**, 10 mmol), g-C_3N_4 (100 mg), and EtOH (50 mL) for 3 h under the refluxing condition (Scheme 3). After purification without using column chromatography, the chromeno[2,3-*b*]pyridine (**4a**) was obtained in 82% yield. The excellent yield allowed this methodology to be used at the industrial level.

A comparative table of various reported catalysts with that of graphitic carbon nitride has been listed in Table 5 (Table 5 reports the synthesis of compound **4a**). The reported procedure for the synthesis of chromeno[2,3-*b*]pyridine (**4a**) utilizes homogeneous bases and uneconomical metal catalysts. Separation and reusability are the major drawbacks of utilizing homogeneous catalysts. Although heterogeneous catalysts are used for the synthesis of chromeno[2,3-*b*]pyridine, the cost factor and metal contamination in the product as well as in the environment are the limitations that are to be noted. Therefore, employing g-C_3N_4 as a catalyst would be a remarkable aspect in the synthesis of chromeno[2,3-*b*]-pyridines as it is inexpensive, metal-free, heterogeneous, easily reusable, and avoids metal contamination in the final products. Hence, the present methodology is economically and environmentally viable.

Encouraged by the successful preparation of chromeno[2,3-*b*]pyridine derivatives in good to high yields, the catalytic application of graphitic carbon nitride was further investigated toward the synthesis of benzylpyrazolyl coumarin derivatives (Table 6). To understand the optimum reaction conditions with regard to solvent, time, temperature, and amount of catalyst, phenyl hydrazine (**5a**), ethyl acetoacetate (**6a**), benzaldehyde (**7a**), and 4-hydroxycoumarin (**8a**) were chosen as the model substrates (Table 6). Initially, the reaction was performed with g-C_3N_4 (10 mg) as a catalyst under solvent-free heating reaction condition (SFRC), but a low amount of yield (32%) was furnished, which further led to the study of different solvent conditions. Therefore, to obtain high yields, a series of green solvents such as ethylene glycol (EG), poly(ethylene glycol) (PEG), H_2O, EtOH, and EtOH/H_2O (1:1) mixture were implemented under the heating condition

Scheme 2. Proposed Mechanism for the Synthesis of Chromeno[2,3-*b*]pyridine Derivatives

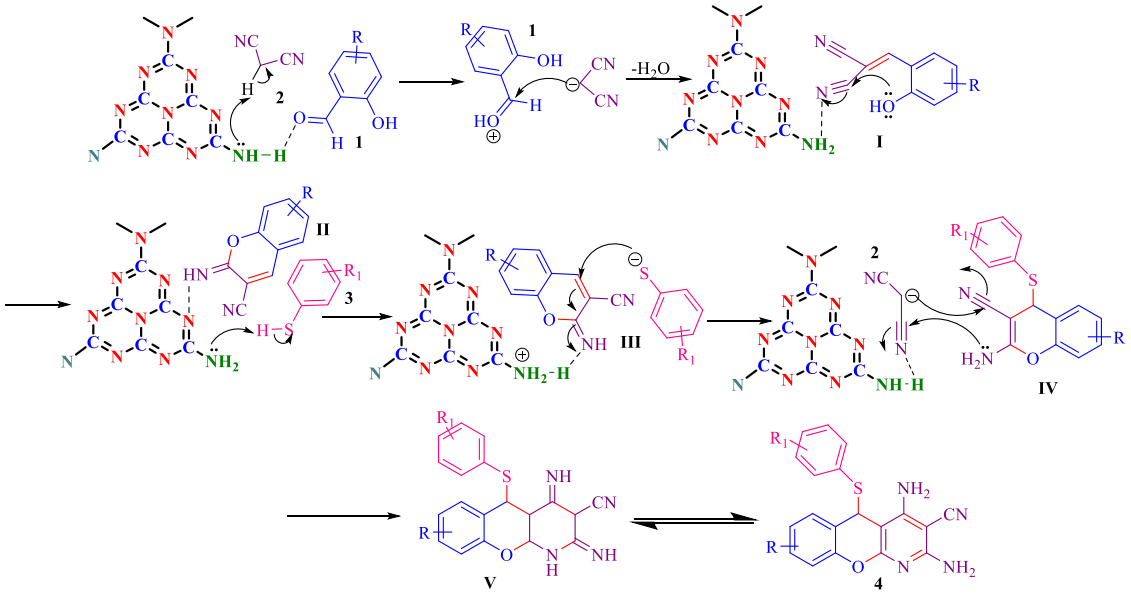

https://doi.org/10.1021/acsomega.2c06070
ACS Omega 2022, 7, 48087−48099

Scheme 3. Gram-Scale Synthesis of Chromeno[2,3-*b*]pyridine

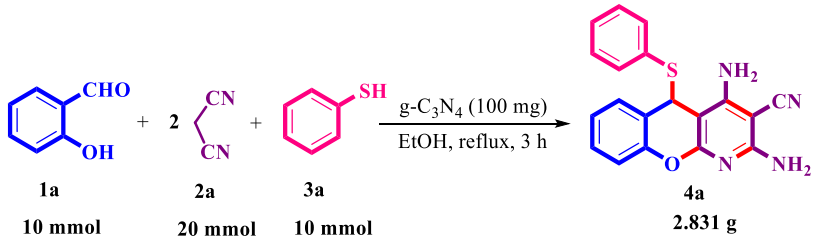

Table 5. Comparative Table of the Reported Catalyst with That of g-C_3N_4 for the Synthesis of Chromeno[2,3-*b*]pyridine (4a)

entry	catalyst	solvent	temperature	time	yield (%)
1	ZrP_2O_7[23]	ethanol	reflux	50 min	90
2	chitosan@citric acid[27]	ethanol	reflux	35 min	92
3	Fe_3O_4@ SiO_2-NH_2[51]	ethanol:H_2O (1:1)	reflux	45 min	94
4	pyridine[52]	ethanol	reflux	2−6 h	75
5	K_2CO_3[26]	ethanol:H_2O (1:1)	reflux	3 h	92
6	Et_3N[25]	ethanol	reflux	3−3.5 h	86
7	SnO NPs[24]	ethanol	reflux	60	88
8	g-C_3N_4	ethanol	reflux	3 h	84

(60 °C), rendering 68, 38, 68, 76, and 70% yields, respectively, in 5 h (Table 6). Therefore, applying EtOH as a solvent of choice, the impact of temperature (30−70 °C) on the model reaction was analyzed. It was observed that the best yield of product was obtained at 60 °C. Further, a decrease in temperature deteriorated the yield, whereas an increase in temperature had no significant impact on the yield of product formation. In addition, the reaction was conducted under varied catalyst concentrations (0−15 mg) (Table 6). To our observation, 10 mg of the catalyst was the optimum condition producing 76% yield in 5 h, and a significant decrease in the yield percentage was obtained on decreasing the catalyst concentration and no remarkable increase in yield was achieved on increasing the catalyst concentration (Table 6). Again, the reaction time was also increased to 6 h, but no improvement in product yield was observed and the yield was found to be 76%. Moreover, various catalysts such as Et_3N, Na_2CO_3, Cs_2CO_3, and L-proline were examined for the aforementioned synthesis, which gave only 59, 54, 62, and 23% yields, respectively, under the optimized condition (Table 7).

Again, the structure of compound **9a** was established by analyzing FT-IR, ^1H, and ^{13}C NMR spectroscopies.

Under the optimized reaction conditions, a wide range of benzylpyrazolyl coumarin derivatives was synthesized using phenyl hydrazine (**5a**, 1 mmol), ethyl acetoacetate (**6a**, 1 mmol), aldehydes (**7a**, 1 mmol), and 4-hydroxy coumarin (**8a**, 1 mmol) in EtOH at 60 °C utilizing 10 mg of the catalyst. A variety of substituted and unsubstituted aromatic aldehydes containing electron-withdrawing and -donating groups were

Table 6. Optimization of Reaction Conditions for the Synthesis of Benzylpyrazolyl Coumarin Derivatives[a]

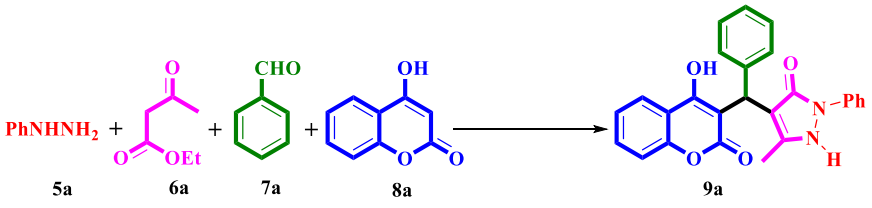

entry	catalyst (mg)	solvent	temperature (°C)	time (h)	yield (%)[b]
1	10	SFRC	60	5	32
2	10	EG	60	5	68
3	10	PEG	60	5	38
4	10	H_2O	60	5	68
5	10	EtOH	60	5	76
6	10	EtOH	60	6	76
7	10	EtOH:H_2O (1:1)	60	5	70
8	10	EtOH	60	4	67
9	10	EtOH	50	6	69
10	10	EtOH	30	18	62
11	8	EtOH	60	5	72
12	5	EtOH	60	5	58
13	15	EtOH	60	5	76
14	nil	EtOH	60	5	24
15	10	EtOH	70	5	76

[a]Reaction conditions: phenyl hydrazine (**5a**, 1 mmol), ethyl acetoacetate (**6a**, 1 mmol), benzaldehyde (**7a**, 1 mmol), and 4-hydroxycoumarin (**8a**, 1 mmol), g-C_3N_4, and solvent (3 mL). [b]Isolated yield.

https://doi.org/10.1021/acsomega.2c06070
ACS Omega 2022, 7, 48087−48099

Table 7. Comparison of Different Catalysts[a]

entry	catalyst (10 mg)	time (h)	yield (%)[b]
1	Et_3N	5	59
2	Na_2CO_3	5	54
3	Cs_2CO_3	5	62
4	L-proline	5	23
5	g-C_3N_4	5	76

[a]Reaction conditions: phenyl hydrazine (**5a**, 1 mmol), ethyl acetoacetate (**6a**, 1 mmol), benzaldehyde (**7a**, 1 mmol), and 4-hydroxycoumarin (**8a**, 1 mmol), catalyst (10 mg), and solvent (3 mL). [b]Isolated yield.

examined for the synthesis of the said compounds (Table 8). Aromatic aldehydes having electron-withdrawing groups such as nitro (−NO_2), cyano (−CN), chloro (−Cl), and bromo (−Br) at different positions of the ring were well tolerated in the reaction and furnished the corresponding products in good yields. However, aromatic aldehydes having electron-donating groups such as methoxy (−OMe) and methyl (−CH_3) groups required a longer reaction time to afford the desired products in moderate yields (Table 8). Moreover, disubstituted benzaldehyde and 2-napthaldehyde were also found to react smoothly to give the products in 76 and 72% yields,

Table 8. Substrate Scope[a]

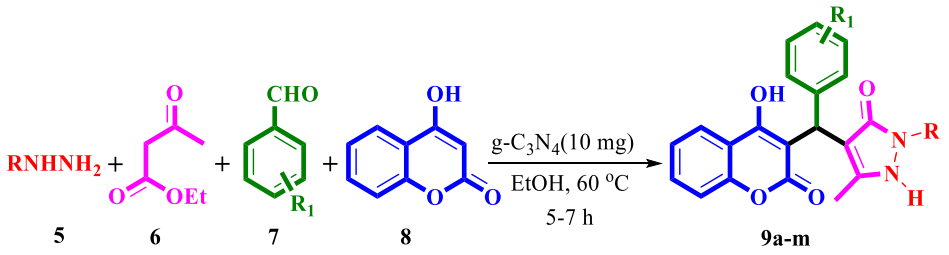

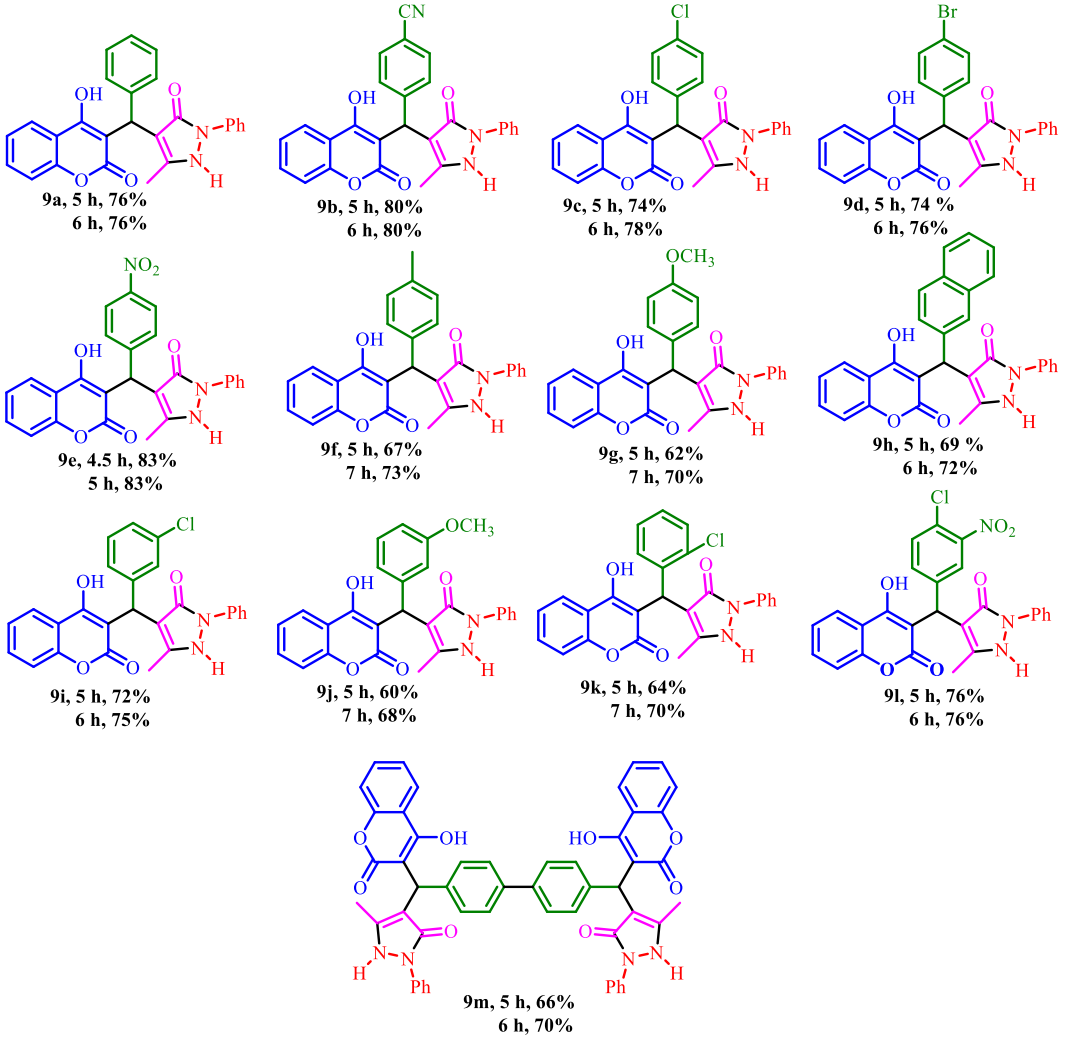

[a]Reaction conditions: phenyl hydrazine (**5**, 1 mmol), ethyl acetoacetate (**6**, 1 mmol), aldehydes (**7**, 1 mmol), 4-hydroxycoumarin (**8**, 1 mmol), g-C_3N_4 (10 mg), EtOH (3 mL), 60 °C for 5−7 h.

https://doi.org/10.1021/acsomega.2c06070
ACS Omega 2022, 7, 48087−48099

Scheme 4. Possible Mechanism for the g-C_3N_4 Catalyzed Synthesis of Benzylpyrazolyl Derivatives

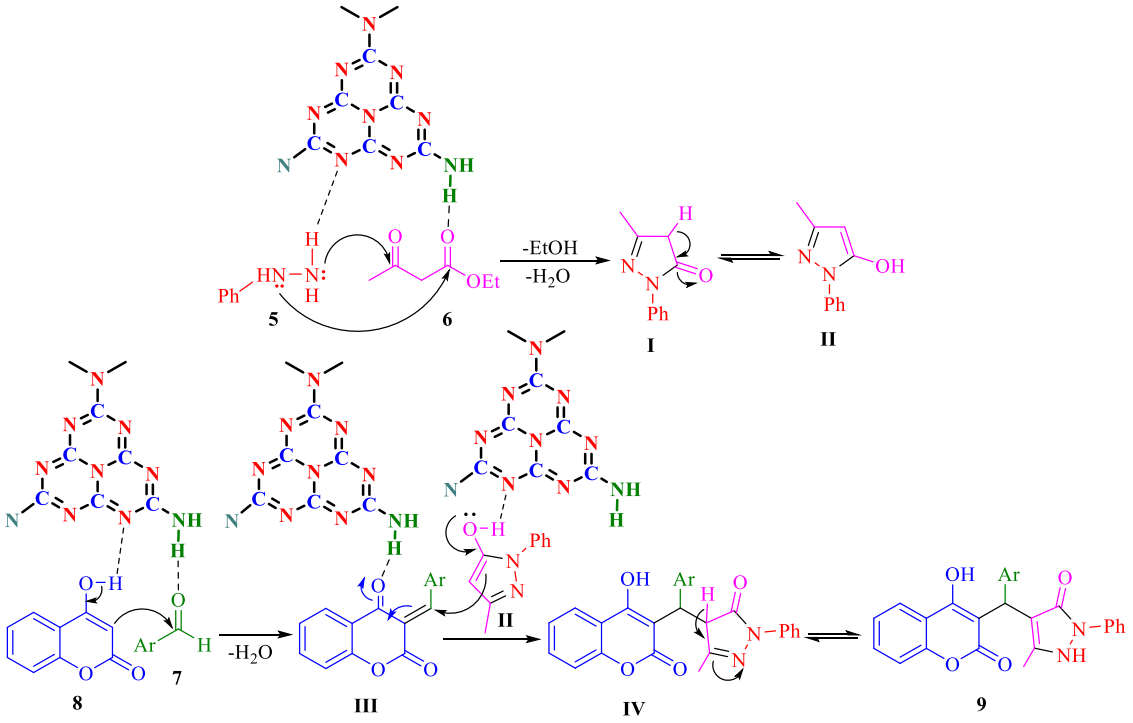

respectively (Table 8). Interestingly, when terepthaldehyde was used in the reaction, a bis-product was obtained in 70% yield (Table 8). The detailed characterization data for the formation of all of the said compounds (**9a−m**) are presented in the Supporting Information.

A possible mechanism for the g-C_3N_4 catalyzed synthesis of benzylpyrazolyl coumarin derivatives is presented in Scheme 4. Initially, phenyl hydrazine (**5**) reacts with ethyl acetoacetate (**6**) in the presence of the g-C_3N_4 catalyst to form the pyrazolone ring (**II**). Then, g-C_3N_4 catalyzed the Knoevenagel reaction between 4-hydroxycoumarin (**8**) and aromatic aldehyde (**7**) furnishing the intermediate (**III**). Then, Michael addition between (**III**) and (**II**) catalyzed by g-C_3N_4 generated a new intermediate (**IV**), which undergoes tautomerization to afford the desired benzylpyrazolyl coumarins (**9**).

Reusability Test. Reusability of the catalyst is an important factor from the economic as well as sustainable point of view. Therefore, the reusability study of the g-C_3N_4 catalyst was examined for the synthesis of chromeno[2,3-*b*]pyridine under the optimized reaction conditions (Table 1). After completion, the reaction mixture was filtered. As both the product and the catalyst are solid, the residue was again dissolved in DMF (3 mL). In DMF, the product is soluble but the catalyst is not; therefore, it was again filtered. The collected catalyst was then washed with water (3 × 10 mL), EtOH (2 × 10 mL), and diethyl ether (2 × 5 mL). Finally, the catalyst was dried and utilized in the next set of reaction under the same optimized reaction condition (Table 1). Furthermore, after separation of the catalyst, 4 mL of H_2O was added to the filtrate (DMF solution), which resulted in precipitation of the product. The obtained precipitate was filtered and washed with H_2O, which was again dried to yield the pure chromeno[2,3-*b*]pyridine product. The experiment was repeated for five consecutive runs, and each run provided a good yield of the product, which showed almost no significant loss in the catalytic activity of g-C_3N_4 (Figure 6). After completion of the reusability test, the reused catalyst was executed for characterization by FT-IR (Figure 7a), TGA (Figure 7b), SEM (Figure 8a), and TEM (Figure 8b) analyses. It was witnessed that the catalyst was able to maintain the morphology and functionalities as the reused and fresh data were in good agreement with each other. On the other hand, a slight decrease in thermal stability of the reused g-C_3N_4 (TGA analysis) was observed.

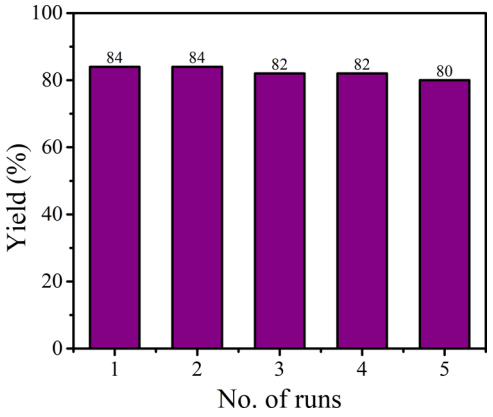

Figure 6. Reusability of the catalyst.

CONCLUSIONS

A new methodology has been developed for the synthesis of biologically relevant chromeno[2,3-*b*]pyridine and benzylpyrazolyl coumarin derivatives via an efficient and heterogeneous graphitic carbon nitride catalyst. In this work, a metal-free, highly stable, and polymeric natured graphitic carbon nitride (g-C_3N_4) was synthesized via simple heating of urea. The prepared g-C_3N_4 was comprehensively characterized by SEM, TEM, EDX, PXRD, FT-IR, and TGA analyses. The prepared g-C_3N_4 showed brilliant catalytic activity toward the synthesis of chromeno[2,3-*b*]pyridines and benzylpyrazolyl coumarin

https://doi.org/10.1021/acsomega.2c06070
ACS Omega 2022, 7, 48087−48099

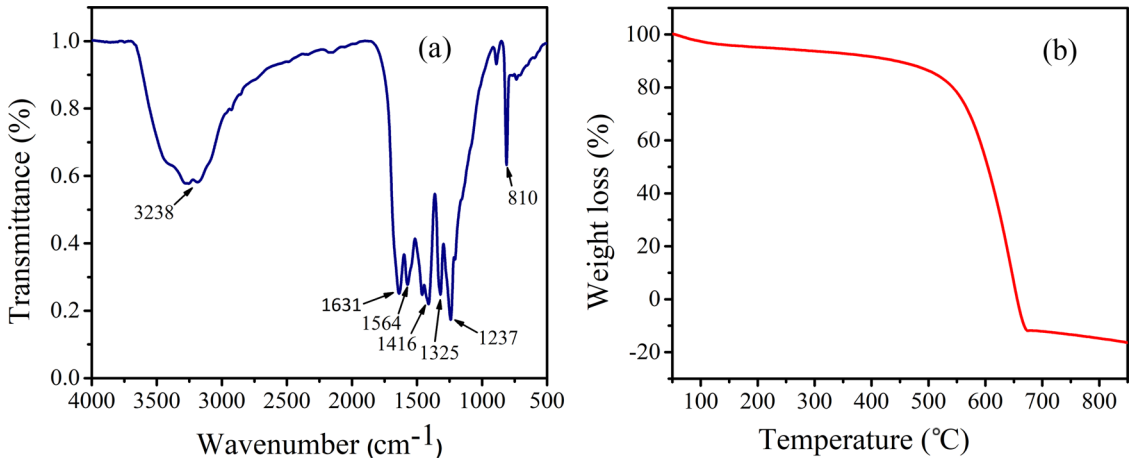

Figure 7. FT-IR spectrum (a) and TGA thermogram (b) of the reused g-C_3N_4.

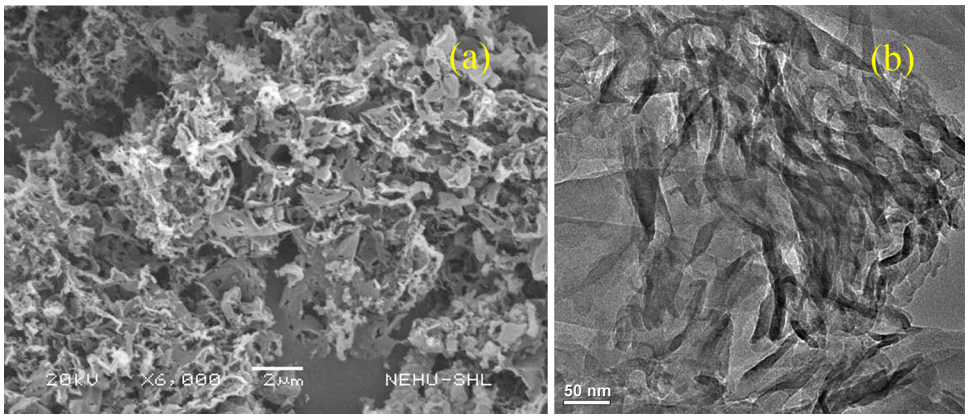

Figure 8. SEM image (a) and TEM image (b) of the reused g-C_3N_4.

derivatives under mild reaction conditions. Various reported procedures utilize homogeneous acids, bases, and expensive metal catalysts for the aforementioned synthesis, whereas our present report has eliminated all of these issues and provided an efficient pathway to synthesize the desired products in good yields under metal-free reaction conditions without the use of additives such as acids and bases. Moreover, the reusability study showed that the catalyst can be reused up to five times without significant loss in its catalytic activity and yield of the product. Gram-scale synthesis was also performed to highlight the importance of the present protocol at the industrial level. Furthermore, this methodology offers column-free purification of chromeno[2,3-*b*]pyridine derivatives. The other advantages of the present method involve (1) use of cheap and readily available starting materials, (2) easy synthetic procedure for catalyst preparation, (3) wide substrate scope, and (4) avoidance of metal contamination in the product as well as in the environment. Moreover, the calculated values of green chemistry metrics are very close to the ideal values, making the methodology sustainable and environmentally viable.

EXPERIMENTAL SECTION

Materials and Methods. Melting points were determined in open capillaries and are uncorrected. Infrared (FT-IR) spectra were recorded on a Bruker Alpha II system (υmax in cm^{-1}) on KBr disks. ^1H NMR and ^{13}C NMR (400, 500 MHz and 100, 125 MHz, respectively) spectra were recorded on Bruker Avance II-400 and JEOL JNM ECS400 spectrometers in DMSO-d_6 and $CDCl_3$ (chemical shifts in δ with TMS as the internal standard). High-resolution mass spectrometry (HRMS) spectra were recorded on a Waters Xevo-G2-XS QT of Mass spectrometer. Transmission electron microscopy (TEM) images were recorded on a JEOL JSM 100CX. Scanning electron microscopy (SEM) and energy-dispersive X-ray (EDX) were recorded on a JSM-6360 (JEOL). Thermogravimetric analysis (TGA) was recorded on a Perkin Elmer Precisely STA 6000 simultaneous thermal analyzer. Powder XRD was recorded on a 9 kW powder X-ray diffraction system (make: Rigaku Technologies, JAPAN, model: Smartlab). Silica gel G (E-Merck, India) was used for TLC. Hexane refers to the fraction boiling between 60 and 80 °C.

Synthesis of Graphitic Carbon Nitride (g-C_3N_4).[49] A total of 10 g of urea was placed in a covered ceramic crucible and heated in a muffle furnace at a temperature of 550 °C for 3 h. After continuous heating for 3 h, the muffle furnace was allowed to be cooled to room temperature, which resulted in the formation of a yellowish mass. The obtained yellowish mass was ground to a fine powder. It was then washed with nitric acid (0.1 mol L^{-1}) and deionized water to remove any residual alkaline impurities (e.g., ammonia) adsorbed on the surface of g-C_3N_4. In the final step, it was dried at 80 °C for 24 h to obtain the pure form of graphitic carbon nitride.

*Synthesis of Chromeno[2,3-b]pyridine Derivatives (**4a–n**).* In a 25 mL round-bottomed flask, a mixture of salicylaldehydes (**1**, 1 mmol), malononitrile (**2**, 2 mmol), and g-C_3N_4 (10 mg) was added to 5 mL of ethanol and

https://doi.org/10.1021/acsomega.2c06070
ACS Omega 2022, 7, 48087−48099

refluxed for 10 min; after that, thiophenol (**3**, 1 mmol) was added to the same reaction mixture and refluxed. The formation of the product was continuously monitored by thin-layer chromatography (TLC). After completion, the precipitate was isolated by filtration. Then, the isolated residue was dissolved in DMF (3 mL) and filtered, and the catalyst was recovered. The filtrate was treated with H_2O (4 mL), which resulted in the precipitation of the products. The desired product (**4**) was then purified by filtration and washing the residue with H_2O (3 × 10 mL) and finally dried under vacuum.

*Synthesis of Benzylpyrazolyl Coumarin Derivatives (**9a–m**).* In a 25 mL round-bottomed flask, a mixture of phenyl hydrazine (**5**, 1 mmol), ethyl acetoacetate (**6**, 1 mmol), g-C_3N_4 (10 mg), and 3 mL of EtOH was taken and stirred at 60 °C for 2 h. After that, aromatic aldehydes (**7**, 1 mmol) and 4-hydroxycoumarin (**8**, 1 mmol) were added to the same reaction vessel, and the reaction mixture was further stirred at 60 °C. After completion of the reaction (TLC), the solvent was removed by filtration and the residue was dissolved in hot methanol (10 mL), which was then filtered to separate the catalyst. Finally, the filtrate was evaporated to dryness and the crude residue was purified by column chromatography over silica gel (60–120 mesh) using ethyl acetate/hexane as the eluent.

Spectral Data of Selected Compounds. *4-Diamino-5-(phenylthio)-5H-chromeno[2,3-b]pyridine-3-carbonitrile (**4a**).*[22] Orange solid. IR (KBr): 3430, 3354, 2203, 1627, 1404 cm^{-1}.

^1H NMR ($CDCl_3$ + DMSO-d_6, 400 MHz): δ = 7.27–7.21 (m, 2H, Ar–H), 7.19 (t, J = 7.6 Hz, 1H, Ar–H), 7.09–7.05 (m, 3H, Ar–H), 6.83 (s, 2H, NH_2), 6.79–6.74 (m, 3H, Ar–H), 6.29 (s, 2H, NH_2), 5.70 (s, 1H, C–H).

^{13}C NMR (DMSO-d_6, 100 MHz): δ = 160.2, 160.1, 156.9, 151.3, 136.4, 131.1, 130.3, 129.9, 129.3, 129.1, 128.8, 128.7, 124.1, 122.2, 117.0, 116.2, 86.6, 70.7, 43.2.

*4-((4-Hydroxy-2-oxo-2H-chromen-3-yl)(phenyl)methyl)-5-methyl-2-phenyl-1H-pyrazol-3(2H)-one (**9a**).*[42] White solid. IR (KBr): 3087, 1654, 1620, 1566, 1494, 1188, 1039, 753 cm^{-1}.

^1H NMR (DMSO-d_6, 500 MHz): δ = 7.74 (d, J = 7.0 Hz, 1H, Ar–H), 7.64 (d, J = 7.5 Hz, 2H, Ar–H), 7.53 (brs, 1H, Ar–H), 7.45 (brs, 2H, Ar–H), 7.31–7.18 (m, 5H, Ar–H), 7.13 (d, J = 5.5 Hz, 3H, Ar–H), 5.64 (s, 1H, C–H), 2.33 (s, 3H, OCH_3).

^{13}C NMR (DMSO-d_6, 125 MHz): δ = 164.7, 164.1, 152.4, 147.4, 140.0, 135.7, 132.3, 129.7, 128.6, 127.2, 127.1, 126.4, 124.2, 121.2, 118.6, 116.3, 107.0, 105.8, 34.1, 10.9.

■ ASSOCIATED CONTENT

Supporting Information

The Supporting Information is available free of charge at https://pubs.acs.org/doi/10.1021/acsomega.2c06070.

Calculation of green chemistry metrics; and analytical and spectral data of ^1H and ^{13}C NMR of all products (PDF)

■ AUTHOR INFORMATION

Corresponding Author

Amarta Kumar Pal − *Department of Chemistry, North-Eastern Hill University, Shillong 793022 Meghalaya, India;* orcid.org/0000-0001-7838-3804; Phone: +91 364 2722606; Email: amartya_pal22@yahoo.com, akpal@nehu.ac.in

Authors

Sushmita Gajurel − *Department of Chemistry, North-Eastern Hill University, Shillong 793022 Meghalaya, India*

Rajib Sarkar − *Department of Chemistry, North-Eastern Hill University, Shillong 793022 Meghalaya, India*

Fillip Kumar Sarkar − *Department of Chemistry, North-Eastern Hill University, Shillong 793022 Meghalaya, India;* orcid.org/0000-0003-4980-1039

Lenida Kyndiah − *Department of Chemistry, North-Eastern Hill University, Shillong 793022 Meghalaya, India*

Complete contact information is available at: https://pubs.acs.org/10.1021/acsomega.2c06070

Author Contributions

†S.G. and R.S. have equal contributions.

Notes

The authors declare no competing financial interest.

■ ACKNOWLEDGMENTS

The authors are thankful to the UGC NEHU-NON NET fellowship and SERB (EMR/2016/005089) for financial assistance. The authors thank the Department of Chemistry, Sophisticated Analytical and Instrumentation Facility (SAIF) of North-Eastern Hill University, Shillong, and the DST-FIST Program (No. SR/FST/CS-II/2019/99 C), Department of chemistry, NEHU. Special thanks to Dr. Ramen Jamatia, Rajiv Gandhi University, Shemphang Hynniewta and Prof. A. K Chandra, NEHU, Shillong, and Samiran Barhoi, Tezpur University.

■ REFERENCES

(1) Dandia, A.; Gupta, S. L.; Saini, P.; Sharma, R.; Meena, S.; Parewa, V. Structure couture and appraisal of catalytic activity of carbon nitride based materials towards sustainability. *Curr. Res. Green Sustainable Chem.* **2020**, *3*, No. 100039.

(2) Dong, G.; Zhang, Y.; Pan, Q.; Qiu, J. A fantastic graphitic carbon nitride (g-C_3N_4) material: Electronic structure, photocatalytic and photoelectric properties. *J. Photochem. Photobiol., C.* **2014**, *20*, 33–50.

(3) Gillan, E. G. Synthesis of nitrogen rich carbon nitride networks from an energetic molecular azide precursor. *Chem. Mater.* **2000**, *12*, 3906–3912.

(4) Sun, Y. P.; Ha, W.; Chen, J. H.; Qi, Y.; Shi, Y. P. Advances and applications of graphitic carbon nitride as sorbent in analytical chemistry for sample treatment: A review. *TrAc, Trends Anal. Chem.* **2016**, *84*, 12–21.

(5) Wang, A.; Wang, C.; Fu, L.; Ng, W. W.; Lang, Y. Recent Advances of Graphitic carbon Nitride-based structures and Applications in catalyst, Sensing, Imaging, and LEDs. *Nano-micro Lett.* **2017**, *9*, No. 47.

(6) Goettmann, F.; Fischer, A.; Antonietti, M.; Thomas, A. Metal-free catalysis of sustainable Friedal-crafts reactions: direct activation of benzene by carbon nitrides to avoid the use of metal chlorides and halogenated compounds. *Chem. Commun.* **2006**, *43*, 4530–4532.

(7) Teter, D. M.; Hemley, R. J. Low compressibility carbon nitrides. *Science* **1996**, *271*, 53–55.

(8) Wang, X.; Maeda, K.; Thomas, A.; Takanabe, K.; Xin, G.; Carlsson, J. M.; Domen, K.; Antoneitti, M. A metal-free polymeric photocatalyst for hydrogen production from water under visible light. *Nat. Mater.* **2009**, *8*, 76–80.

(9) Su, Q.; Sun, J.; Wang, J.; Wang, Z.; Cheng, W.; Zhang, S. Urea-derived graphitic carbon nitride as an efficient heterogeneous catalyst

for CO_2 conversion into cyclic carbonates. *Catal. Sci. Technol.* **2014**, *4*, 1556−1562.
(10) Fidan, T.; Torabfam, M.; Saleem, Q.; Wang, C.; Kurt, H.; Yüce, M.; Tang, J.; Bayazit, M. K. Functionalized Graphitic Nitrides for Environmental and sensing Applications. *Adv. Energy Sustainability Res.* **2021**, *2*, No. 2000073.
(11) Dong, F.; Wu, L.; Sun, Y.; Fu, M.; Wu, Z.; Lee, S. C. Efficient synthesis of polymeric g-C_3N_4 layered materials as novel efficient visible light driven photocatalysts. *J. Mater. Chem.* **2011**, *21*, 15171−15174.
(12) Zheng, Y.; Jiao, Y.; Chen, J.; Liu, J.; Liang, J.; Du, A.; Zhang, W.; Zhu, Z.; Smith, S. C.; Jaroneic, M.; Lu, G. Q.; Qiao, S. Z. Nanoporous Graphitic nitride-C3N4@Carbon Metal-Free Electrocatalysts for Highly Efficient Oxygen Reduction. *J. Am. Chem. Soc.* **2011**, *133*, 20116−20119.
(13) Jin, X.; Balasubramanian, V. V.; Selvan, S. T.; Sawant, D. P.; Chari, M. A.; Lu, G. Q.; Vinu, A. A highly Ordered Mesoporous Carbon Nitride Nanoparticles With High Nitrogen Content: A Metal-Free Basic Catalyst. *Angew. Chem., Int. Ed.* **2009**, *48*, 7884−7887.
(14) Bai, X.; Wang, L.; Zong, R.; Zhu, Y. Photocatalytic Activity Enhanced via g-C_3N_4 Nanoplates to Nanorods. *J. Phys. Chem. C.* **2013**, *117*, 9952−9961.
(15) Ge, L.; Zuo, F.; Liu, J.; Ma, Q.; Wang, C.; Sun, D.; Bartels, L.; Feng, P. Synthesis and Efficient Visible Light Photocatalytic Hydrogen Evolution of Polymeric g-C_3N_4 Coupled With Cds Quantum Dots. *J. Phys. Chem. C* **2012**, *116*, 13708−13714.
(16) (a) Gupta, S.; Khurana, J. M. An efficient approach for the synthesis of 5-hydroxy-chromeno [2,3-b]pyridines under catalyst and solvent free conditions. *Green Chem.* **2017**, *19*, 4153−4156. (b) Elinson, M. N.; Ryzhkova, Y. E.; Ryzhkov, F. Multicomponent design of chromeno[2,3-b]pyridine systems. *Russ. Chem. Rev.* **2021**, *90*, 94−115.
(17) El-Saghier, A. M. M.; Naili, M.; Rammash, B.; Saleh, N.; Kreddan, K. M. Synthesis and anti-bacterial activity of some new fused chromenes. *Arkivoc* **2008**, *2007*, 83−91.
(18) Azuine, M. A.; Tokuda, H.; Takayasu, J.; Enjyo, F.; Mukainaka, T.; Konoshima, T.; Nishino, H.; Kapadia, G. J. Cancer chemopreventive effect of 216 phenothiazines and related tri-heterocyclic analogues analogues in the 12-O-tetradecanoyl-217 phorbol-13 acetate promoted EpsteiBarr virus early antigen activation and the 218 mouse skin two-stage carcinogenesis models. *Pharmacol. Res.* **2004**, *49*, 161−169.
(19) Maruyama, Y.; Goto, K.; Terasawa, M. Method for treatment of Rheumatism. Ger. Offen. D. E 3010751, 19810806. 1981.
(20) Anderson, D. R.; Hegde, S.; Reinhard, E.; Gomez, L.; Vernier, W. F.; Lee, L.; Liu, S.; Sambandam, A.; Snider, P. A.; Masih, L. Aminocyanopyridine inhibitors of mitogen activated protein kinase-activated protein kinase 2 (MK-2). *Bioorg. Med. Chem. Lett.* **2005**, *15*, 1587−1590.
(21) (a) Ukawa, K.; Ishiguro, T.; Kuriki, H.; Nohara, A. Synthesis of the Metabolites and Degradation Products of 2-Amino-7-isopropyl-5-oxo-5H-[1] benzopyrano [2,3-b] pyridine-3-carboxylic Acid (Amoxanox). *Chem. Pharm. Bull.* **1985**, *33*, 4432−4437. (b) Karamshahi, Z.; Ghorbani-Vaghei, R.; Keypour, H.; Rezaei, M. T. Highly efficient synthesis of chromeno[2,3-*b*]pyridine using Graphene-Oxide/N^1,N^3-*bis*(pyridin-2-ylmethyl)propane-1,3-diamine-Copper nanocomposites as a novel catalyst. *Appl. Organomet. Chem.* **2020**, *34*, No. e5737. (c) Ryzhkova, Y. E.; Fakhrutdinov, A. N.; Elinson, M. N. Ammonium Salts of 5-(3-Chromenyl)-5H-chromeno[2,3-*b*]pyridines. *Molbank* **2021**, *2021*, No. M1219.
(22) Evdokimov, N. M.; Kireev, A. S.; Yakovenko, A. A.; Yu, M.; Magedov, A. I. V.; Kornienko, A. One-step synthesis of Heterocyclic Privileged Medicinal Scaffolds by a Multicomponent Reaction of Malononitrile with Aldehydes and Thiols. *J. Org. Chem.* **2007**, *72*, 3443−3453.
(23) Ghomi, J. S.; Kiani, M.; Ziarati, A.; Alavi, H. S. Highly efficient synthesis of benzopyranopyrimidines via ZrP_2O_7 nanoparticles catalyzed multicomponent reactions of salicylaldehydes with malononitrile and thiols. *J. Sulfur Chem.* **2014**, *35*, 450−457.
(24) Safaei-Ghomi, J.; Alavi, H. S.; Baghbahadorani, E. H. SnO nanoparticles as an efficient catalyst for the one-pot synthesis of Chromeno[2,3-b]pyridines and 2-amino-3,5-dicyano-6-sulfanyl pyridines. *RSC Adv.* **2014**, *4*, 50668−50677.
(25) Evdokimov, N. M.; Kireev, A. S.; Yakovenko, A. A.; Yu, M.; Magedov, A. I. V.; Kornienko, A. One-step synthesis of Heterocyclic Privileged Medicinal Scaffolds by a Multicomponent Reaction of Malononitrile with Aldehydes and Thiols. *J. Org. Chem.* **2007**, *72*, 3443−3453.
(26) Mishra, S.; Ghosh, R. K_2CO_3-Mediated, one pot, Multicomponent synthesis of Medicinally Potent Pyridine and Chromeno-[2,3-b]pyridine Scaffolds. *Synth. Commun.* **2012**, *42*, 2229−2244.
(27) Safaei-Ghomi, J.; Tavazo, M.; Vakili, M. R.; Alavi, H. S. Chitosan functionalized by citric acid: an efficient catalyst for one-pot synthesis of 2,4-diamino-5H-[1]benzopyrano[2,3-b]pyridine-3-carbonitriles 5-(arylthio) or 5-[(arylmethyl)thio] substituted. *J. Sulfur Chem.* **2017**, *38*, 236−248.
(28) Saha, A.; Payra, S.; Banerjee, S. One-pot multicomponent synthesis of highly functionalized bio-active pyrano[2,3-c]pyrazole and benzylpyrazolyl coumarin derivatives using ZrO_2 nanoparticles as a reusable catalyst. *Green Chem.* **2015**, *17*, 2859−2866.
(29) Jung, J. C.; Jung, Y. J.; Park, O. S. A Convenient One-Pot Synthesis of 4-hydroxy coumarin, 4-hydroxythiocoumarin and 4-hydroxyquinolin-2(1H)-One. *Synth. Commun.* **2001**, *31*, 1195−1200.
(30) Hesse, S.; Kirsch, G. A rapid access to coumarin derivatives (using Vilsmier Haack and Suzuki-cross coupling reaction). *Tetrahedron Lett.* **2002**, *43*, 1213−1215.
(31) Lee, B. H.; Clothier, M. F.; Dutton, F. E.; Conder, G. A.; Johnson, S. S. Anthelmintic *β*-hydroxyketoamides (BKAS). *Bioorg. Med. Chem. Lett.* **1998**, *8*, 3317−3320.
(32) Melagraki, G.; Afantitis, A.; Markopoulou, O. I.; Detsi, A.; Koufaki, M.; Kontogiorgis, C.; Litina, D. J. H. Synthesis and evaluation of the antioxidant and anti-inflammatory activity of novel coumarin-3-aminoamides and their alpha-lipoic acid adducts. *Eur. J. Med. Chem.* **2009**, *44*, 3020−3026.
(33) Jung, J.-C.; Lee, J.-H.; Oh, S.; Lee, J.-G.; Park, O.-S. Synthesis and anti-tumour activity of 4-hydroxycoumarin derivatives. *Bioorg. Med. Chem. Lett.* **2004**, *14*, 5527−5531.
(34) Pasha, F. A.; Muddassar, M.; Neaz, M. M.; Cho, S. J. Pharmacophore and docking-based combined in-silico study of KDR inhibitors. *J. Mol. Graphics Modell.* **2009**, *28*, 54−61.
(35) Badawey, E. S. A.; El-Ashmawey, I. M. Nonsteroidal anti-inflammatory agents-Part 1: Antiinflammatory, analgesics and antipyretic activity of some new 1-(pyrimidin-2-yl)-3-pyrazolin-5ones and 2-(pyrimidin-2-yl)-1,2,4,5,6,7-hexahydro-3H-indazol-3-ones. *Eur. J. Med. Chem.* **1998**, *33*, 349−361.
(36) Moreau, F.; Desroy, N.; Genevard, J. M.; Vongsouthi, V.; Gerusz, V.; Fralliec, G. L.; Oliveira, C.; Floquet, S.; Denis, A.; Escaich, S.; Wolf, K.; Busemann, M.; Aschenbsenner, A. Discovery of new Gram-negative antivirulence drugs: structure and properties of novel *E. coli* WaaC inhibitors. *Bioorg. Med. Chem. Lett.* **2008**, *18*, 4022−4026.
(37) Rosiere, C. E.; Grossman, M. I. An analog of Histamine that stimulates Gastric Acid Secretion without Other Actions of Histamine. *Science* **1951**, *113*, No. 651.
(38) Himly, M.; Schmid, B. J.; Pittertschatscher, K.; Bohle, B.; Grubmayr, K.; Ferreira, F.; Ebner, H.; Ebner, C. J. IgE-mediated immediate-type hypersensitivity to the pyrazolone drug propyphenazone. *J. Allergy Clin. Immunol.* **2003**, *111*, 882−888.
(39) Watanabe, T.; Yuki, S.; Egawa, M.; Nishi, H. Protective effects of MCI-186 on cerebral ischemia: possible involvement of free radical scavenging and antioxidant actions. *J. Pharmacol. Exp. Ther.* **1994**, *268*, 1597−1604.
(40) Watanabe, K.; Tanaka, M.; Yuki, S.; Hirai, M.; Yamamoto, Y. Protective effects of MCI-186 on cerebral ischemia: Possible involvement of free radical scavenging and antioxidant actions. *J. Clin. Biochem. Nutr.* **2018**, *62*, 20−38.

https://doi.org/10.1021/acsomega.2c06070
ACS Omega 2022, 7, 48087−48099

(41) Wu, T. W.; Zeng, L. H.; Wu, J.; Fung, K. P. Myocardial protection of MCI-186 in rabbit ischemia-reperfusion. *Life Sci.* **2002**, *71*, 2249−2255.
(42) Ghosh, P. P.; Pal, G.; Paul, S.; Das, A. R. Design and synthesis of benzylpyrazolyl coumarin derivatives via a four component reaction in water: investigation of the weak interactions accumulating in the crystal structure of a signified compound. *Green Chem.* **2012**, *14*, 2691−2698.
(43) Chate, A. V.; Shaikh, B. A.; Bondle, G. M.; Sangle, S. M. Efficient atom-economic one-pot multicomponent synthesis of benzylpyrazolyl coumarins and novel pyrano[2,3-c]pyrazoles catalysed by 2-aminoethanesulfonic acid (taurin) as a bioorganic catalyst. *Synth. Commun.* **2019**, *49*, 2244−2257.
(44) Yaragorla, S.; Pareek, A.; Dada, R. Ca(II)-catalyzed, one-pot four synthesis of functionally embellished benzylpyrazolyl coumarins in water. *Tetrahedron Lett.* **2015**, *56*, 4770−4774.
(45) Kamble, N. R.; Kamble, V. T. A Facile Solvent-Free Route for one-pot Multicomponent synthesis of Benzylpyrazolyl coumarin derivatives in presence of effective synergistic catalytic systems. *Asian J. Chem.* **2019**, *31*, 1357−1361.
(46) Mahdizadeh Ghohe, N.; Tayebee, R.; Amini, M. M. Synthesis and characterization of mesoporous Nb-Zr/KIT-6 as a productive catalyst for the synthesis of benzylpyrazolyl coumarins. *Mater. Chem. Phys.* **2019**, *223*, 268−276.
(47) Kim, M.; Hwang, S.; Yu, J. S. Novel ordered nanoporous graphitic C_3N_4 as a support for Pt-Ru anode catalyst in direct methanol fuel cell. *J. Mater. Chem.* **2007**, *17*, 1656−1659.
(48) Choudhary, P.; Bahuguna, A.; Kumar, A.; Dhankhar, S. S.; Nagaraja, C. M.; Krishnan, V. Oxidized graphitic carbon nitride as a sustainable metal-free catalyst for hydrogen transfer reactions under mild conditions. *Green Chem.* **2020**, *22*, 5084−5095.
(49) Sharma, P.; Sasson, Y. Highly active g-C_3N_4 as a solid base catalyst for knoevenagel condensation reaction under phase transfer conditions. *RSC Adv.* **2017**, *7*, 25589−25596.
(50) Wang, H.; Yuan, X.; Wu, Y.; Zeng, G.; Chen, X.; Leng, L.; Li, H. Synthesis and applications of novel graphitic carbon nitride/metal-organic frameworks mesoporous photocatalyst for dyes removal. *Appl. Catal., B.* **2015**, *174*−*175*, 445−454.
(51) Ghasemzadeh, M. A.; Basir, M. H. A.; Babaei, M. Fe_3O_4@SiO_2-NH_2 core-shell nanocomposite as an efficient and green catalyst for the multicomponent synthesis of highly substituted chromeno[2,3-b]pyridines in aqueous ethanol media. *Green Chem. Lett. Rev.* **2015**, *8*, 40−49.
(52) Gan, H. F.; Cao, W. W.; Fang, Z.; Li, X.; Tang, S. G.; Guo, K. Efficient synthesis of chromenopyridine and chromene via MCRs. *Chin. Chem. Lett.* **2014**, *25*, 1357−1362.

https://doi.org/10.1021/acsomega.2c06070
ACS Omega 2022, 7, 48087−48099